Author Manuscript

Author Manuscript

Author Manuscript

Author Manuscript

HHS Public Access

Author manuscript

Trans Soc Min Metall Explor Inc. Author manuscript; available in PMC 2018 March 19.

Published in final edited form as:

Trans Soc Min Metall Explor Inc. 2017 ; 342(1): 72–82. doi:10.19150/trans.8110.

Experimental study on foam coverage on simulated longwall roof

W.R. Reed, **Y. Zheng**, **S. Klima**, **M.R. Shahan**, and **T.W. Beck**

Research mining engineer, associate service fellow, mining engineer, mechanical engineer and research engineer, respectively, Centers for Disease Control and Prevention, National Institute for Occupational Safety and Health (CDC-NIOSH), Pittsburgh Mining Research Division, Pittsburgh, PA, USA

Abstract

Testing was conducted to determine the ability of foam to maintain roof coverage in a simulated longwall mining environment. Approximately 27 percent of respirable coal mine dust can be attributed to longwall shield movement, and developing controls for this dust source has been difficult. The application of foam is a possible dust control method for this source. Laboratory testing of two foam agents was conducted to determine the ability of the foam to adhere to a simulated longwall face roof surface. Two different foam generation methods were used: compressed air and blower air. Using a new imaging technology, image processing and analysis utilizing ImageJ software produced quantifiable results of foam roof coverage. For compressed air foam in 3.3 m/s (650 fpm) ventilation, 98 percent of agent A was intact while 95 percent of agent B was intact on the roof at three minutes after application. At 30 minutes after application, 94 percent of agent A was intact while only 20 percent of agent B remained. For blower air in 3.3 m/s (650 fpm) ventilation, the results were dependent upon nozzle type. Three different nozzles were tested. At 30 min after application, 74 to 92 percent of foam agent A remained, while 3 to 50 percent of foam agent B remained. Compressed air foam seems to remain intact for longer durations and is easier to apply than blower air foam. However, more water drained from the foam when using compressed air foam, which demonstrates that blower air foam retains more water at the roof surface. Agent A seemed to be the better performer as far as roof application is concerned. This testing demonstrates that roof application of foam is feasible and is able to withstand a typical face ventilation velocity, establishing this technique's potential for longwall shield dust control.

Keywords

Foam coverage; Dust control; Longwall roof

Disclaimer

The findings and conclusions in this presentation are those of the authors and do not necessarily represent the views of NIOSH. Mention of any company name, product, or software does not constitute endorsement by NIOSH.

Author Manuscript Author Manuscript Author Manuscript Author Manuscript

Introduction

U.S. National Institute for Occupational Safety and Health (NIOSH) personnel have visited many longwall operations at various geographical locations in the United States, conducting benchmark surveys to characterize current operating practices and dust control measures in use. Sources of respirable dust generated from the longwall face have been identified as: (1) intake, 10 percent, (2) stage loader, 20 percent, (3) shields, 27 percent, and (4) shearer, 43 percent (Rider and Colinet, 2011). Dust generated by the shearer, armored face conveyor and stage loader can mainly be controlled by water sprays and increases in ventilation air quantities. However, research has demonstrated limited effective controls for dusts generated by shield movements (Rider and Colinet, 2006).

One possible approach to mitigating shield dust generation is to apply a layer of water or foam to the shield-roof interface at the area between the shield tip and the longwall face. Once this interface is blanketed with foam or water, dust will be less likely to become airborne and contaminate the airways over the personnel walkways when shields move over it. Though water is an abundant and common dust control measure, roof applications have limited success because water is unable to remain in place in adequate quantities for the necessary duration between application and shield advance. Past and current testing of foam for material properties has shown that it has longer applicability times, ranging from 10 to 60 min (Reed, Beck et al., 2017) and better performance for dust control, ranging from 19 to 96 percent improved efficiency over water (Salyer, 1970; Wojtowicz, 1974; Hiltz, 1975; Singh and Laurite, 1984; Bhaskar and Gong, 1992). The majority of this foam dust control research has focused on dust control efficiency at the longwall shearer or continuous miner cutting drum, not on the mine roof.

Discussions with personnel familiar with longwall operations have revealed that the time frame for the longwall shearer passing a particular shield and its shield advance is between one and three minutes. Therefore, under the worst-case condition, the foam coating effect will need to last for a minimum of three minutes. The current research evaluates the ability of foam to cover and remain suspended from the mine roof to maintain the required moisture on the mine roof surface over the estimated three-minute time period of shield advance.

Experimental design

Test facility

Full-scale laboratory tests at NIOSH's Pittsburgh laboratory were conducted to quantify the ability of a prototype foam generating apparatus to deliver foam to a simulated mine roof and the ability of the foam to adhere to the roof. Figure 1 shows the section of the foam roof application, with height of 1.98 m (6.5 ft), width of 1.98 m (6.5 ft) and length of 6.1 m (20 ft). The roof was made of black painted plywood with roof markers 2.54 cm (1 in.) and 5.1 cm (2 in.) high to aid in determining foam coverage.

When applied in an actual mining situation, the foam generator and spray nozzle are planned to be mounted on the longwall shearer. Application of the foam to the mine roof will proceed as the shearer moves along its cut. To represent the movement of the shearer-

Author Manuscript Author Manuscript Author Manuscript Author Manuscript

mounted foam spray, a linear actuator was used to move the foam spray carriage along a rail on the floor of the mine roof simulator. The movement of the foam spray carriage was controlled at a constant velocity to represent shearer movement, using the linear actuator's computer-controlled setup.

Foam was sprayed from the carriage onto the roof to determine its ability to be applied to the roof, to determine the duration of the life of the foam and to quantify coverage once applied. The results of this testing will be used in establishing foam as a useful dust control tool in longwall mining. To quantify the foam roof coverage, digital image analysis was used for foam evaluation using ImageJ, a free software developed by the U.S. National Institutes of Health. The digital image was obtained by a remote-controlled camera located in the middle of the traveling course adjacent to the track to get maximum image coverage of the test area (Fig. 1).

Test parameters

Many of the parameters of this testing were held constant to ensure that testing proceeded efficiently while obtaining the desired results. They include shearer tram speed, water pressure, foam concentration, incident ventilation air velocity, distance from foam nozzle to mine roof, angle of application and nozzles.

Tram speeds for Caterpillar's shearer with the smallest diameter of 1.6 m (63 in.) are 0.48 m/s (94 fpm) maximum and 0.24 (47 fpm) minimum at maximum pull of 97 t (107 st) (Caterpillar, 2013). As the foam would only be applied during cutting, a tram speed of 0.20 m/s (40 fpm) was selected for evaluation. A Parker Hannifin HLE80c linear actuator with a Parker 6K2 controller (Parker Hannifin, Cleveland, OH) was used to tram the foam nozzle through the 6.1-m (20-ft)-long foam testing section.

Previous foam property testing determined the optimum water pressure. For foam generated by compressed air, the water pressure was maintained at a constant 0.28 MPa (40 psi) with the air pressure at 0.21 MPa (30 psi). For foam generated by blower air, the water pressure was set at 0.21 MPa (30 psi) with the blower air set at half power/speed (30 Hz) (Reed et al., 2017).

In previously conducted foam property tests, the desired foam properties were obtained with foam agent concentrations ranging from 2 to 3 percent (Reed, Beck et al., 2017). Two agents were tested in this roof application study: (1) a butyl diglycol nonionic foam agent, referred to as agent A, and (2) a sodium alpha olefin sulfonate anionic foam agent, referred to as agent B. The foam concentration targeted this range, and variations of concentrations were not tested.

Longwall panels must be ventilated to achieve a minimum airflow of 14.16 m^3/s (30,000 cfm) under Title 30 of the Code of Federal Regulations (U.S. Mine Safety and Health Administration, MSHA, 2014). The airflow velocities required to control methane and respirable dust are to be specified in the ventilation plan at locations within 15.2 m (50 ft) and 30.4 m (100 ft) of the headgate and the tailgate (MSHA, 2014). Therefore, airflow velocities are an important parameter to be evaluated. Initial testing was conducted in an

Author Manuscript Author Manuscript Author Manuscript Author Manuscript

area of no airflow movement to evaluate the viability of foam to be applied to the roof. Once the no-flow condition results were analyzed, and residence times established, the test setup was then evaluated with 3.3 m/s (650 fpm) face ventilation airflow, which is the average longwall airflow velocity according to a NIOSH survey (Rider and Colinet, 2011). To obtain maximum coverage of the mine roof, foam spray angle to the mine roof and distance from nozzle to roof were adjusted based upon the geometry of the spray coverage and the dimensions of the section. Differing the spray angles and nozzle distances from the mine roof were not tested. For this test, the nozzle distance from the mine roof was kept constant at approximately 0.91m (3 ft). Additionally, through preliminary testing, a nozzle was deemed necessary in order to obtain the optimum coverage of the foam spray to the mine roof. For compressed air foam, a Spraying Systems H3/4U VeeJet nozzle (Spraying Systems Co., Glendale Heights, IL) was used. For blower air foam, a brass nozzle that fits the foam hose was used, resulting in partial roof area coverage along the width of the roof marker. To improve coverage, two 3D-printed nozzles were designed. Therefore, three nozzles were tested for blower air foam: (1) Spraying Systems VeeJet 2U-502000 brass nozzle, (2) 3D-printed nozzle 1 and (3) 3D-printed nozzle 2.

For compressed air foam, all parameters were held constant except for the foam agent and ventilation airflow. For blower air foam, the foam agent, ventilation airflow and nozzle type were varied.

Experimental cases

Two foam generation methods were tested: compressed air and blower air. To generate the compressed air foam, a Lafferty 916105 HV foamer (Lafferty Equipment Manufacturing Inc., North Little Rock, AR) was used. Blower-generated foam was created using a NIOSH-developed foam generator.

For compressed air foam, tests of four different test conditions were completed, each repeated three times: (1) agent A without ventilation, (2) agent A with 3.3 m/s (650 fpm) ventilation, (2) agent B without ventilation and (4) agent B with 3.3 m/s (650 fpm) ventilation. The testing evaluated the foam at 0, 3 and 30 min. Two out of the three times were 30 min long, with the third one lasting three min. Twelve tests were conducted.

For the blower air foam, tests of the same four different test conditions were completed for each nozzle type. From previous compressed air foam generator data analysis, it was concluded that there was no statistical difference in coverage at either 0 m/s (0 fpm) or 3.3 m/s (650 fpm). In the present study, 0 m/s (0 fpm) was only tested in one trial for agent A and one trial for agent B for comparison purposes. Twenty-four tests were completed to evaluate the foam at 0, 3 and 30 min.

Additionally, throughout all of the tests, lighting conditions were held constant. Foam property tests were conducted before each tram of the foam nozzle after the foam was stabilized from the foam producer.

Author Manuscript Author Manuscript Author Manuscript Author Manuscript

Data analysis

Photographs were taken of the selected area at 0, 3 and 30 min, after which the images were analyzed with ImageJ, a commonly used program (Ferreira and Rasband, 2010; Ozbayoglu, Akin and Eren, 2007; Rami-shojaei, Vachier and Schmitt, 2009; Tarimala et al., 2013), to get the percentage of dark areas, or areas without foam coverage. The results evaluated the effects of factors such as residence time, foam agent type and ventilation velocity. Figure 2 shows the procedures of the first two steps. Detailed procedures for photo processing can be found in Reed, Zheng et al. (2017).

Results and discussion

The individual results of testing of the compressed air foam are summarized in Table 1. In Table 1, picture identification parameters are an abbreviation of the test trial illustrating the name of the agent, ventilation condition, time duration of the foam, and the test number of the test condition. For example, B_650fpm_3m_t2 means the foam agent is B with 3.3 m/s (650 fpm) ventilation, measurement taken at three minutes, and it is the second of three tests of the test condition. The column for the total dark spot area sums up the area of all of the black regions in square inches from the image. The fourth column in the table is the percentage of dark area compared with the total image area, which is approximately 4,555 cm^2 (706 $in.^2$) for the compressed air foam and 4,452 cm^2 (690 $in.^2$) for the blower air foam. This is the percentage of no- or low-foam region inside the total image area. The lower the percentage, the better the foam coverage. All analyses focused on the total dark spot area measurement in that this provides a representation of the quality of foam coverage. Typical images obtained during compressed air foam testing are presented in Figs. 3, 4, 5 and 6. Table 2 presents the resultant data processed by the ImageJ software.

Foam properties of each test are also included in Table 1. These properties include foam expansion ratio, foam drainage accumulation, and time. Foam expansion ratio is determined by calculating the ratio of the foam collection vessel's volume and the final foamable liquid volume collected during the foam stability tests using the following equation:

$$Expansion = \frac{Vol_{empty}}{Weight_{full} - Weight_{empty}}$$

where $Expansion$ is the expansion of the foam, Vol_{empty} is the known volume of the empty collection vessel, $Weight_{\text{full}}$ is the weight of the full collection vessel filled with foam, and $Weight_{\text{empty}}$ is the weight of the empty collection vessel.

Foams with higher expansion ratios are considered more desirable than foams with low expansion ratios. Foam drainage accumulation is determined by the collection of water from the foam collection vessel at consistent time intervals of two minutes up to approximately 10 min after filling the test flask. Time is the actual total time over which the drainage accumulation occurred. Attempts were made to keep the time as close to 10 min as possible. Details of foam drainage calculation procedures can be found in Reed, Beck et al. (2017).

Author Manuscript Author Manuscript Author Manuscript Author Manuscript

Foams with lower values of foam water loss are more desirable than foams with higher values.

The individual results of blower air foam testing are summarized in Table 3. The picture identification parameter was modified to include the nozzle type. For example, Brass Nozzle_B_650 fpm_3m_t2 means the nozzle type is brass, the foam agent is B with 3.3 m/s (650 fpm) ventilation, measurement taken at three minutes, and it is the second of three tests of the test condition. The total image area for the blower air foam tests was remeasured to be approximately 4,452 cm^2 (690 sq in.) for the whole area. All other descriptions defined for compressed air foam are the same for the blower air foam tests. Images for blower air foam are similar to that of compressed air foam. Therefore, blower air foam images are not presented but can be found in Reed, Zheng et al. (2017).

Discussion of foam properties

Reviewing the foam properties from the compressed air foam testing, the foam expansion ratios and drainage appear to be relatively consistent for both foam agents. Agent B's expansion ratio ranged from 10.68 to 13.77 with drainages ranging from 85 to 115 mL over approximately 10 min. Agent A's expansion ratio ranged from 9.48 to 11.74 with drainages ranging from 19 to 31 mL over 10 min. While their expansion ratios are comparable, agent A has much less drainage, which means it is able to retain more water than agent B. The ability to retain more water should make it more desirable as far as foam structure is concerned.

In reviewing the foam properties from the blowing air foam testing, the foam expansion ratios and drainage appear to change dramatically for both foam agents. Agent B's expansion ratio ranges from 11.6 to 90.5 with drainages ranging from 3 to 88 mL over approximately 10 min. Agent A's expansion ratio ranges from 12.6 to 43.8 with drainages ranging from 0 to 7 mL over 10 min. As with the compressed air foam testing, agent A has much less drainage.

Compared with the previously used compressed air foam generator with foam expansion ratios ranging from 9.5 to 13.8, this blower air type of foam generator can produce relatively higher foam expansion ratios, as high as 90.5. The design of this blower system seems to be able to force more air into the foam agent-water solution and produce higher expansion foam. The higher expansion ratio could potentially lower the cost of foam with the same amount of foam required for dust control. The current problem with the blower air foam system is the coverage of foam on the roof is not consistent. This may need to be addressed for future dust control testing.

Past literature from U.S. Bureau of Mines (USBM) contracts cited expansion ratios ranging from 150 to 280. These ratios were obtained using air-aspirated nozzles with water pressures of 0.83 MPa (120 psi) (Wojtowicz, 1974). Expansion ratios ranging from 52 to 400 have been obtained using blower-generated foam (Salyer, 1970). The China University of Mining and Technology has tested the generation of air-aspirated foam. However, the water pressures were extremely high, ranging from 3.2 to 7.6 MPa (460 to 1,110 psi), and

Author Manuscript Author Manuscript Author Manuscript Author Manuscript

development of a custom-designed nozzle was required to generate foam using air aspiration. This high-pressure water induced airflows into the nozzle ranging from 23.95 to 36.36 m^3/h (14.1 to 21.4 cfm), producing a foam with an expansion ratio of approximately 60 (Wang, 2013). Each case stated that foams with these expansion ratio properties were adequate to control respirable dust from coal cutting operations.

Discussion of application results for compressed air foam

Measurements of foam thickness generated by compressed air were not quantified during testing. However, observations showed that the foam layered with a “dimpling” effect, as shown in Fig. 2b. The foam did not apply in an even layer as anticipated. The dimpling effect is caused by gravity acting as a downward force on the foam. Several random measurements of foam thickness showed that the foam layer thickness ranged from 1.27 to 2.54 cm (0.5 to 1.0 in.) but was 0.0 in. where dark spots occurred. Observations during testing showed that this range of thickness was consistent throughout all tests.

Effect of face ventilation velocity

In comparing the foam coverage for face ventilation velocities of 0 m/s (0 fpm) with that of 3.3 m/s (650 fpm), no statistical difference is seen in coverage at either velocity. Table 4 summarizes the results of the face ventilation velocity comparison using a two-tailed *t*-test. These results show that the foam coverage data at 0 m/s (0 fpm) and 3.3 m/s (650 fpm) face ventilation velocities are not statistically different for both A and B foam agents.

Effect of time interval

The review of the compressed air foam roof application results focuses on foam coverage as determined by the total dark spot area by image analysis and on the time interval from the initial application. The time intervals evaluated are from initial application to 3 min after, and to 30 min after. The 0 min to 3 min time interval is to represent the time it takes for the shield to move once the shearer has passed that shield. The 0 min to 30 min interval is to examine the durability of the foam to endure.

In evaluating the results from the previous tables, the average total dark spot area represents the area not covered by foam. Therefore, foam coverage quality increases as the average total dark spot area decreases. Agent A has better foam coverage than agent B when comparing average total dark spot areas with their corresponding time intervals.

It is noticed that the area of dark spots increases as the time interval increases. This represents the decay of the foam. In conducting a statistical analysis of the decay for agent A with 0 m/s (0 fpm) face ventilation from 0 min to 3 min, there is no statistical difference in comparing the results over this time period using a two-tailed *t*-test — $T(4) = 1.28$, $p = 0.27$. For agent A with 3.3 m/s (650 fpm) face ventilation from 0 min to 3 min, there also is no statistical difference in comparing the results over this time period using a two-tailed *t*-test — $T(4) = 1.73$, $p = 0.16$. The comparison of 0 min to 30 min demonstrates a statistical difference over this time period at both face ventilation velocities of 0 m/s (0 fpm) — $T(3) = 9.86$, $p = 0.002$ — and 3.3 m/s (650 fpm) — $T(3) = 5.60$, $p = 0.01$. These results show that for agent A, there is no difference in foam coverage from initial application to 3 min.

Author Manuscript Author Manuscript Author Manuscript Author Manuscript

However, there is a difference in foam coverage from initial application to 30 min and from 3 min to 30 min due to decay of the foam over time. At 30 min, the average dark spot area was 276.45 cm^2 (42.85 $in.^2$) for 0 m/s (0 fpm) ventilation and 239.87 cm^2 (37.18 $in.^2$) for 3.3 m/s (650 fpm), and 94 to 95 percent of the foam was still intact.

The evaluation of agent B yields results similar to those for agent A. In conducting a statistical analysis of the decay for agent B from 0 min to 3 min, there is no statistical difference in comparing the results over this time period using a two-tailed *t*-test at 0 m/s (0 fpm) — $T(4) = 1.30$, $p = 0.26$ — and 3.3 m/s (650 fpm) — $T(4) = 2.07$, $p = 0.11$. The comparison of 0 min to 30 min demonstrates a statistical difference in the comparison over this time period at both face ventilation velocities of 0 m/s (0 fpm) — $T(3) = 17.00$, $p = 0.0002$ — and 3.3 m/s (650 fpm) — $T(3) = 17.46$, $p = 0.0004$. These results show that agent B is similar to agent A in that there is no difference in foam coverage from initial application to 3 min. However, there is a difference in foam coverage from initial application to 3 min and from 3 min to 30 min due to the decay of the foam over time. At 30 min, the average dark spot area was 4,109.15 cm^2 (636.92 $in.^2$) for 0 m/s (0 fpm) ventilation and 3,641.48 cm^2 (564.43 in^2) for 3.3 m/s (650 fpm). Note that these areas are approaching the limit of 4,554.83 cm^2 (706 $in.^2$), the area of analysis — with almost 80 to 90 percent of all the foam having decayed.

Effect of foam agent type

In comparing the foam coverage by foam agent type, there is no statistical difference in coverage at the initial application for face ventilation velocities of 0 m/s (0 fpm) and 3.3 m/s (650 fpm). For the 3-min time interval, there is no statistical difference in coverage when the face ventilation velocity is 0 m/s (0 fpm). However, with a 3.3 m/s (650 fpm) face ventilation velocity, there is a statistical difference in coverage between agents A and B, with agent A having better coverage. For the 30-min time interval, there is a statistical difference in coverage between agents A and B for both face ventilation airflows of 0 m/s (0 fpm) and 3.3 m/s (650 fpm), with agent A having better coverage. The average dark spot area for agent A was 276.43 cm^2 (42.85 $in.^2$) for 0 m/s (0 fpm) ventilation and 239.86 cm^2 (37.18 $in.^2$) for 3.3 m/s (650 fpm), compared with 4,109.15 cm^2 (636.92 $in.^2$) for 0 m/s (0 fpm) ventilation and 3,641.48 cm^2 (564.43 $in.^2$) for 3.3 m/s (650 fpm) for agent B.

These results (Table 1) show that upon initial application, both foam agents covered the roof well. As time progressed, agent A had better roof coverage, especially with a face ventilation airflow velocity of 3.3 m/s (650 fpm). It is indeterminable at this time how this coverage translates to effective dust control, but it is expected that better coverage would correlate with better dust control performance.

Discussion of application results for blower air foam

Measurements of foam thickness during testing were not quantified. However, observations of the foam from the 3D-printed nozzle 1 showed that its foam thickness could be between 1.27 and 2.54 cm (0.5 and 1 in.). The foam from the other two nozzles — the brass nozzle and the 3D-printed nozzle 2 — can be thicker, between 7.62 and 12.70 cm (between 3 and 5 in.) at the beginning of the roof application test. However, due to the light weight of the

Author Manuscript Author Manuscript Author Manuscript Author Manuscript

foam, it was easily blown away during the test instead of clinging to the roof and collapsing upon itself at the same spot. Roof coverage from the brass nozzle and the 3D-printed nozzle 2 was not adequate to cover the test areas. The 3D-printed nozzle 1 did have adequate roof coverage due to its wider spray angle, showing that spray coverage was dependent upon nozzle design.

From Table 3, the expansion ratio of foam from the 3D-printed nozzle 1 ranges from 11.6 to 28.2, which is much less than those of foam from the 3D-printed nozzle 2, which ranges from 26.2 to 72.9, and foam from the brass nozzle, which ranges from 36.7 to 90.5. The dimpling effect, mentioned earlier, caused by gravity acting as a downward force on the foam, was apparent for the 3D-printed nozzle 1 but was not observed for the other two nozzles.

The sprays from the nozzles were not consistent within the three trials under the same conditions. The mounting of the nozzle to the moving actuator was not as stationary as the compressed air mounting due to the large 5.08-cm (2-in.) hose diameter that connected the nozzle to the foam generator, and due to the wriggling and twisting motion of the long hose, which was 15.2 m (50 ft) in length, during actuator movement. This motion resulted in movement of the nozzle, which changed the angle of spray toward the roof. This also resulted in foam coverage being changed for each trial when the spray did not cover the whole image processing area. Due to the fact that the nozzles can only deliver foam to cover part of the roof and the inconsistency of the coverage for each trial, the data were normalized by subtracting the initial conditions. This method normalizes the area of analysis to the area coverage for each nozzle, which eliminates any inconsistency of foam application due to changes in spray angle caused by the bulky large-diameter hoses.

Effect of agent type

A comparison of the foam coverage of foam agents A and B was conducted at a ventilation airflow of 3.3 m/s (650 fpm). At the 3-min time interval, no statistical difference was found in coverage between agents A and B using the 3D-printed nozzle 1 and the brass nozzle. For the 3D-printed nozzle 2, there was a statistical difference, with agent A having better coverage. The average dark spot area was 198.90 cm^2 (30.83 $in.^2$) for agent A and 388.77 cm^2 (60.26 $in.^2$) for agent B. Approximately 93 percent of the agent A foam was still intact while approximately 83 percent of the agent B foam was intact. At the 30-min time interval, there was a statistical difference in coverage between agents A and B for all the nozzle types, with agent A always having better coverage. For the 3D-printed nozzle 1, the average dark spot area was 344.77 cm^2 (53.44 $in.^2$) for agent A and 2,093.93 cm^2 (324.56 $in.^2$) for agent B. Approximately 92 percent of the agent A foam was still intact, while approximately 50 percent of the agent B foam was intact. For the 3D-printed nozzle 2, the average dark spot area was 742.00 cm^2 (115.01 $in.^2$) for agent A and 1,538.90 cm^2 (238.53 $in.^2$) for agent B. Approximately 74 percent of the agent A foam was still intact, while approximately 33 percent of the agent B foam was intact. For the brass nozzle, the average dark spot area was 381.16 cm^2 (59.08 $in.^2$) for agent A and 3,031.86 cm^2 (469.94 $in.^2$) for agent B. Approximately 88 percent of the agent A foam was still intact, while approximately 5 percent of the agent B foam was intact. It should be noted that in all percentages, the amount

Author Manuscript Author Manuscript Author Manuscript Author Manuscript

of foam agent intact is based upon the amount of foam applied by each specific nozzle. The foam percent intact was calculated using the following equation:

$$\%\text{intact} = 1 - [\text{normalized dark spot area} / ((4,451.60\ \text{cm}^2 \text{ or } 690\ \text{in.}^2) - \text{average dark spot area at 0 min})] \times 100$$

Effect of nozzle type

In comparing the foam coverage by nozzle type, three nozzles were used at a ventilation airflow of 3.3 m/s (650 fpm). For agent A, there were statistical differences in coverage between the 3D-printed nozzles 1 and 2 and between the 3D-printed nozzle 2 and the brass nozzle at the 3-min interval. The 3D-printed nozzle 2 had the poorest foam coverage, 198.90 cm^2 (30.83 $in.^2$). No statistical difference was found in coverage between the 3D-printed nozzle 1 and the brass nozzle. At the 30-min time interval, there was no statistical difference in coverage among any of the nozzles.

Similar results were found for agent B. There were statistical differences in coverage between the 3D-printed nozzles 1 and 2 and between the 3D-printed nozzle 2 and the brass nozzle at the 3-min interval. The 3D-printed nozzle 2, again, had the poorest foam coverage, 388.77 cm^2 (60.26 $in.^2$). At the 30-min time interval, there were no statistical differences in coverage between the 3D-printed nozzles 1 and 2 and between the 3D-printed nozzle 1 and the brass nozzle. There was statistical significance between the 3D-printed nozzle 2 and the brass nozzle, showing that there is a difference between the two data sets. In this case, the 3D-printed nozzle 2 had better coverage, with 1,538.90 cm^2 (238.53 $in.^2$), than the brass nozzle, with 3,031.86 cm^2 (469.94 $in.^2$).

Conclusions

The results of this study demonstrate that application of foam to the mine roof is technically feasible. Quantifying the foam coverage on the mine roof is important, especially for longwall mining dust control. The foam must have the ability to stay on the roof for longwall mining shield dust control. Digital analysis of pictures of roof coverage will quantify the coverage of the foam, permitting comparisons of images over time. This analysis should indicate the better foam agent for longwall shield dust control by showing which agent has the better coverage, allowing the mining entity to select the better foam agent.

The compressed air foam generator uses a small device that uses compressed air, water and foam agent, mixing them to generate consistent foam. A nozzle is necessary in order to obtain a good spray pattern for application. It is important that the nozzle size or diameter be as close to the diameter of the delivery hose as possible to minimize breakdown of the foam. From observations and data analysis, roof application to the mine roof is technically feasible with the Laffertey foam generator.

Another method used a blower to generate foam. NIOSH's prototype blower foam generator requires water, blower-generated air and a foaming agent to create the foam. Three types of nozzles were tested. Originally a Spraying Systems VeeJet 2U-502000 brass nozzle was used. Knowing that the nozzle opening should be close to the hose diameter to prevent

Author Manuscript Author Manuscript Author Manuscript Author Manuscript

destruction of the foam, two 3D-printed nozzles (1 and 2) were designed and built in an attempt to improve foam application. From the observation and data analysis, it can be concluded that the application of foam to the mine roof is technically feasible with this blower foam generator.

Roof application testing was conducted using image analysis techniques to determine quality of coverage. Throughout testing, the foam properties were consistent, with agent A having less water drainage than B. These results were consistent with previous foam property testing completed at NIOSH (Reed et al., 2017). It was found that compressed air foam is easier to apply to the mine roof than blower air foam. This is due to the fact that blower air foam requires larger-diameter hoses — a minimum of 5.08 cm (2 in.) for blower foam compared with 2.54 cm (1 in.) for compressed air foam. These larger hoses are bulkier than and not as flexible as the smaller-diameter hoses, making it difficult to maintain proper spray angle and consistent foam coverage during application. Also, there are fewer spray nozzle types available for the larger size, thus requiring in-house nozzle design and construction for foam application. Nevertheless, application of these foam generators to a longwall system should translate well, as the entire foam system — generator and nozzle — would move with the longwall shearer. This would require less hose length and would increase stability, unlike the current study's laboratory setup, where the foam generator was stationary with only the nozzle moving, requiring more than 15.2 m (50 ft) of hose.

The image analysis results for compressed air foam showed that ventilation airflow did not have an impact on the foam application. Comparing the results from zero ventilation velocity to 3.3 m/s (650 fpm) did not show any statistical significance for either foam agent. The length of time after foam application did have statistical significances as the time interval approached 30 min. The average dark spot area increased as the time interval increased. The image analysis did show that there were differences in the roof application between foam agents A and B. Agent A seemed to apply and sustain better than agent B, especially in 3.3 m/s (650 fpm) ventilation airflow. These results showed that at 3 min, 98 percent of foam A was intact, while 95 percent of foam agent B was intact. At 30 min, 94 percent of foam A was intact, while only 20 percent of foam agent B was intact.

Image analysis of the blower air foam was conducted using data from the test with 3.3 m/s (650 fpm) ventilation. The effect of foam agent type on roof coverage showed that at the 3-min time interval, no statistical difference was found in coverage between agent A and agent B using the 3D-printed nozzle 1 and the brass nozzle. There was a statistical difference in coverage using the 3D-printed nozzle 2, with agent A having better coverage — 93 percent of the foam intact compared with 83 percent of the foam intact for agent B. At the 30-min time interval, there was a statistical difference in coverage between agents A and B for all the nozzle types, with agent A having better coverage.

The effect on roof coverage due to nozzle type was also analyzed. For agent A, at the 3-min time interval, there were statistical differences in coverage between the 3D-printed nozzles 1 and 2 and between the 3D-printed nozzle 2 and brass nozzle, with the 3D-printed nozzle 2 having the worst coverage. No statistical difference was found in coverage between the 3D-printed nozzle 1 and the brass nozzle. At the 30-min time interval, there was no statistical

Author Manuscript Author Manuscript Author Manuscript Author Manuscript

difference in coverage among the nozzles. Similar results were found for agent B at 3 min. There were statistical differences in coverage between the 3D-printed nozzles 1 and 2 and between the 3D-printed nozzle 2 and the brass nozzle, with the 3D-printed nozzle 2 having the worst coverage. However, at the 30-min time interval, the 3D-printed nozzle 2 had better coverage than the brass nozzle.

Overall, these roof coverage results show that agent A may perform better, especially over long time periods. However, agent B may perform just as well, as these results do not represent any dust control ability between the two foam agents. The nozzle type is an important factor to consider for foam application. The nozzle opening area should be as close to the hose opening area as possible to prevent destruction of the foam as it is applied to the mine roof. Additionally, spray angle is important to set and maintain, in order to keep full application to the area being controlled: the area between the shield tip and the face. Spray angle can be optimally set using materials to support the nozzle that can withstand the stresses caused by the compressed air foam hose and the bulky large-diameter hoses used for blower foam generation. As a result of the work from this study, application of foam to the mine roof for shield dust control is technically viable.

References

Bhaskar R, Gong R. Effect of foam surfactants on quartz and dust levels in continuous miner sections. Mining Engineering. 1992 Sep.:1164–1168.

Caterpillar. Brochure from website. 2013. CAT EL2000 Longwall Shearer.

Ferreira, T., Rasband, WS. ImageJ User Guide — IJ 1.46. 2010. p. 2010-2012.http://www.imagej.nih.gov/ij/docs/guide

Hiltz, RH. MSA Research Corp. U.S. Department of the Interior, Bureau of Mines; Washington, DC: 1975. Underground Application of Foam for Suppression of Respirable Dust. (USBM contract #:H0133034), Research report for U.S. Bureau of Mines OFR-24-76

Mine Safety and Health Administration (MSHA). Title 30 of the Code of Federal Regulations (30 CFR), Part 75.325 (c) (1) and (2) Air Quantity. U.S. Department of Labor, U.S. Government Printing Office, Office of the Federal Register; Washington, DC: 2014.

Ozbayoglu EM, Akin S, Eren T. Image processing techniques in foam characterization. Energy Sources, Part A: Recovery, Utilization, and Environmental Effects. 2007; 29(13):1175–1185.

Rami-shojaei S, Vachier C, Schmitt C. Automatic analysis of 2D foam sequences: Application to the characterization of aqueous proteins foams stability. Image and Vision Computing. 2009; 27:609–622. https://doi.org/10.1016/j.imavis.2008.10.004.

Reed, WR., Beck, TW., Zheng, Y., Klima, S., Driscoll, J. Material Property Tests of Foam Agents to Determine Their Potential for Longwall Mining Dust Control Research. SME Annual Conference & Expo; Feb. 19–22, 2017; Denver, CO. Englewood, CO: Society for Mining, Metallurgy & Exploration; 2017. Preprint 17-082

Reed, WR., Zheng, Y., Klima, S., Shahan, M., Beck, T. Assessing foam application to mine roof for longwall mining shield dust control. SME Annual Conference & Expo; Feb. 19–22; Denver, CO. Englewood, CO: Society for Mining, Metallurgy & Exploration; 2017. Preprint 17-013

Rider JP, Colinet JF. Benchmarking longwall dust control technology and practices. Mining Engineering. 2011; 63(9):74–80.

Rider, JP., Colinet, JF. Dust control on longwalls – Assessment of the state-of-the-art. Proceedings of the 11th U.S./North American Mine Ventilation Symposium; June 5–7, 2006; State College, PA. 2006. p. 225-232.

Salyer, IO., Sun, SM., Schwendeman, JL., Wurstner, AL. USBM Contract Final Report, Contract No. HO100179. U.S. Department of the Interior, Bureau of Mines; 1970. Foam Suppression of Respirable Coal Dust.

Author Manuscript Author Manuscript Author Manuscript Author Manuscript

Singh, MM., Laurite, AW. Field tests of a foam dust-suppression system with longwall shearers. In: Peng, SS., editor. Proceedings of the Coal Mine Dust Conference; Morgantown, WV. Oct. 8–10; West Virginia University; 1984. p. 101-109.

Tarimala, S., Fillipo, B., Smokers, A., Usher, C. Quantitative Performance Assessment of New Foam Control Agents in Waterborne Coatings. 2013 European Coatings Show; Nuremberg, Germany. Mar. 19–21, 2013; 2013.

Wojtowicz, A., Mueller, JC., Hedley, WH., Schwendeman, JL., Sun, S. USBM Contract Final Report, Contract No. H0111351. Department of the Interior, Bureau of Mines; 1974. Foam Suppression of Respirable Coal Dust.

Wang H, Wang D, Wang Q, Jia Z. Novel approach for suppressing cutting dust using foam on a fully mechanized face with hard parting. Journal of Occupational and Environmental Hygiene. 2013; 11(3):154–164. https://doi.org/10.1080/15459624.2013.848039.

Author Manuscript Author Manuscript Author Manuscript Author Manuscript

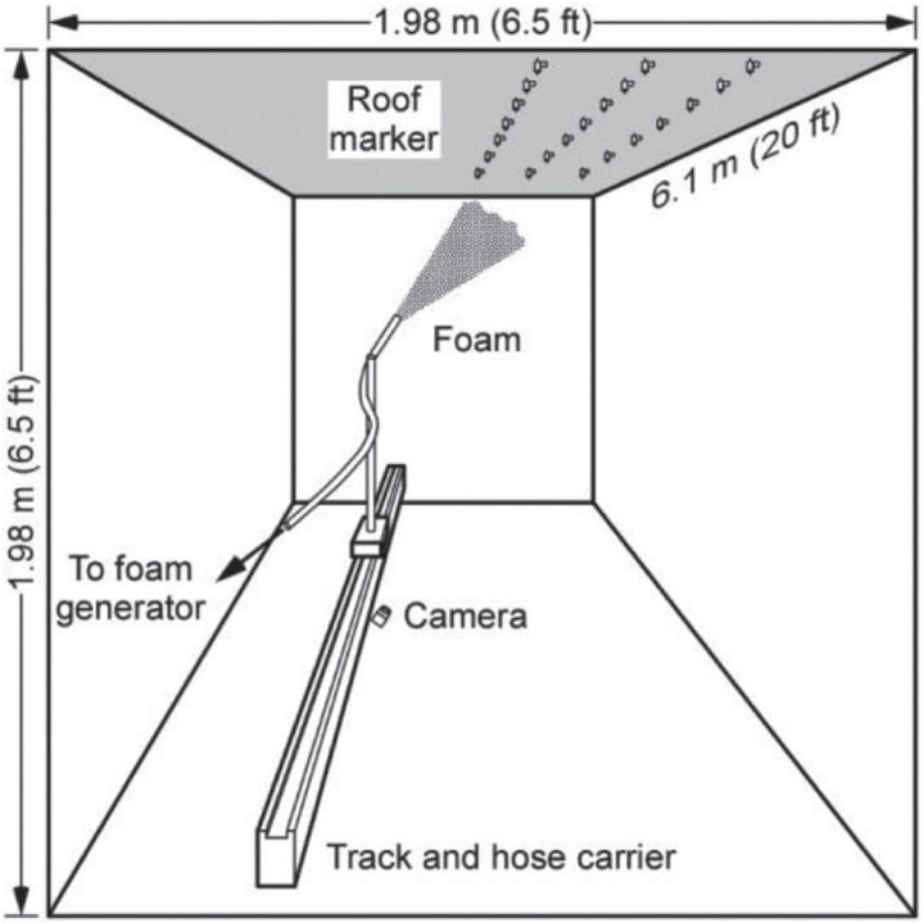

Figure 1.
Mine roof simulator for foam application (not to scale). The roof construction is black painted plywood.

Author Manuscript Author Manuscript Author Manuscript Author Manuscript

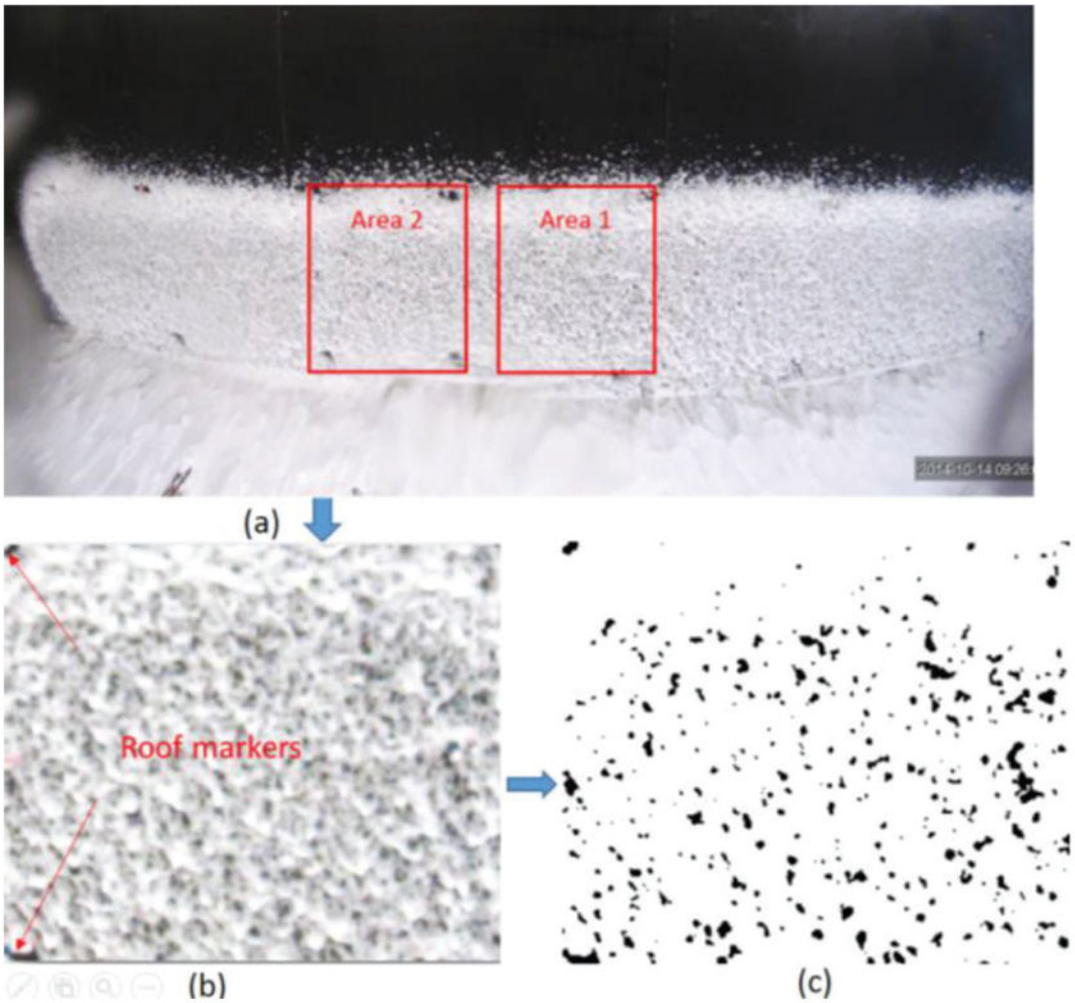

Figure 2.
Photo analysis process: (a) Picture during the test showing the two possible areas for image processing, (b) selected area bounded by roof markers and known distances and (c) image processed by ImageJ.

Author Manuscript Author Manuscript Author Manuscript Author Manuscript

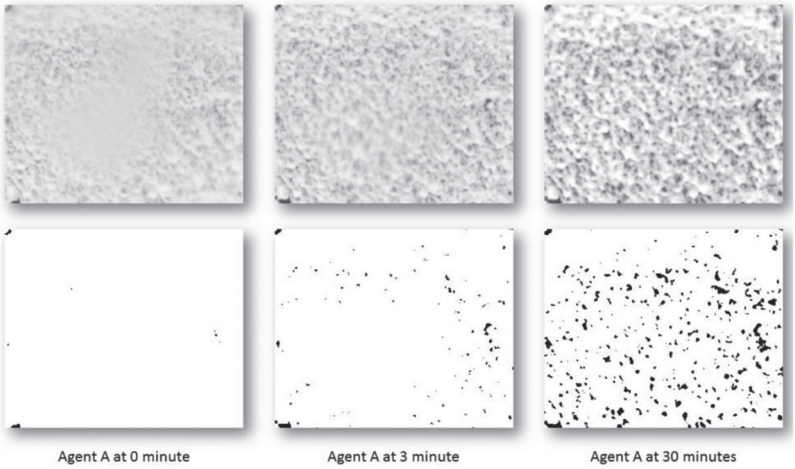

Figure 3.
Images obtained for agent A compressed air foam at 0 m/s ventilation (test 3).

Author Manuscript Author Manuscript Author Manuscript Author Manuscript

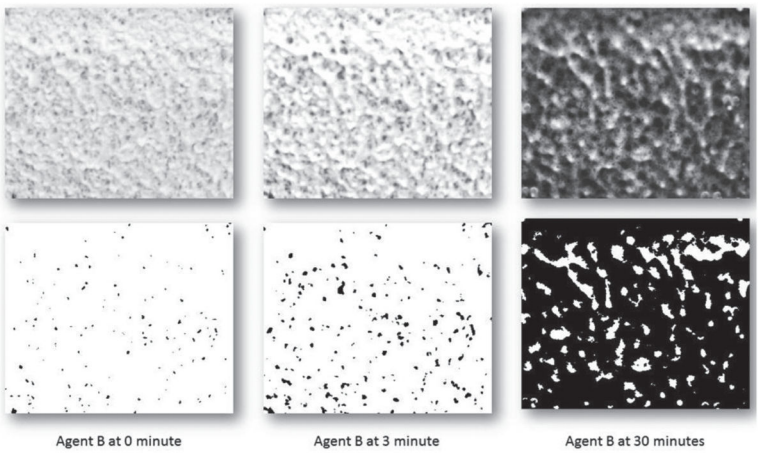

Figure 4.
Images gathered for agent B compressed air foam at 0 m/s ventilation (test 1).

Author Manuscript Author Manuscript Author Manuscript Author Manuscript

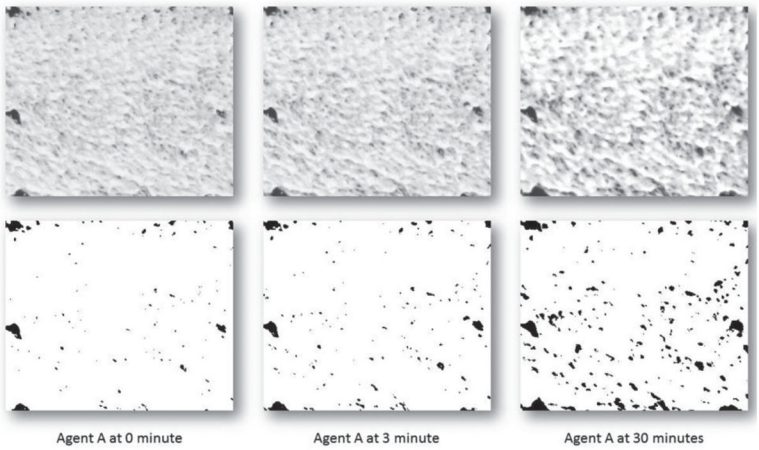

Figure 5.
Images gathered for agent A compressed air foam at 3.3 m/s (650 fpm) ventilation (test 13).

Author Manuscript Author Manuscript Author Manuscript Author Manuscript

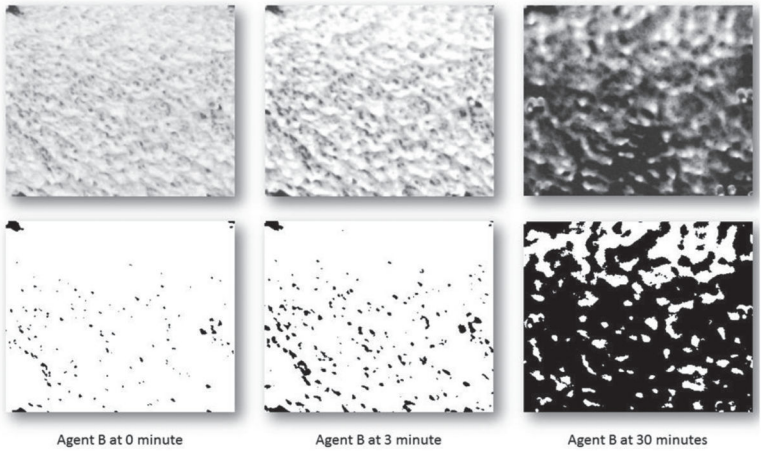

Figure 6.
Images gathered for agent B compressed air foam at 3.3 m/s (650 fpm) ventilation (test 6).

Author Manuscript Author Manuscript Author Manuscript Author Manuscript

Trans Soc Min Metall Explor Inc. Author manuscript; available in PMC 2018 March 19.

Table 1

Summary of the image analysis results for compressed air foam.

Test no.	Picture identification parameters	Total dark spot area (cm^2 / $in.^2$)	Percent of dark area	Foam expansion ratio	Drainage accumulation (mL)	Time (hh:mm:ss)
3	A_0fpm_0m_t1	4.92 / 0.76	0.11	10.52	28	0:09:55
	A_0fpm_3m_t1	36.83 / 5.71	0.81			
	A_0fpm_30m_t1	267.86 / 41.52	5.88			
9	A_0fpm_0m_t2	51.25 / 7.94	1.13	10.80	27	0:09:59
	A_0fpm_3m_t2	78.19 / 12.12	1.72			
10	A_0fpm_0m_t3	63.76 / 9.88	1.40	9.71	31	0:09:15
	A_0fpm_3m_t3	119.99 / 18.60	2.64			
	A_0fpm_30m_t3	284.99 / 44.17	6.26			
4	A_650fpm_0m_t1	72.30 / 11.21	1.59	11.44	19	0:09:47
	A_650fpm_3m_t1	94.75 / 14.69	2.08			
	A_650fpm_30m_t1	200.66 / 31.10	4.41			
13 *	A_650fpm_0m_t2	73.26 / 11.36	1.61	11.74	25	0:09:22
	A_650fpm_3m_t2	106.08 / 16.44	2.33			
	A_650fpm_30m_t2	279.06 / 43.26	6.13			
12	A_650fpm_0m_t3	46.11 / 7.15	1.32	9.48	28	0:09:05
	A_650fpm_3m_t3	66.99 / 10.38	1.92			
1	B_0fpm_0m_t1	37.39 / 5.80	0.82	11.55	106	0:09:59
	B_0fpm_3m_t1	164.44 / 25.49	3.61			
	B_0fpm_30m_t1	3,685.22 / 599.11	84.92			
5	B_0fpm_0m_t2	348.80 / 54.06	7.66	10.68	109	0:09:27
	B_0fpm_3m_t2	728.40 / 112.90	16.00			
	B_0fpm_30m_t2	4,353.09 / 674.73	95.64			
7	B_0fpm_0m_t3	100.50 / 15.58	2.21	11.33	107	0:09:45
	B_0fpm_3m_t3	342.78 / 53.13	7.53			
2	B_650fpm_0m_t1	67.81 / 10.51	1.49	13.77	85	0:11:29
	B_650fpm_3m_t1	209.40 / 34.01	4.82			
	B_650fpm_30m_t1	3,386.98 / 524.98	74.67			
6	B_650fpm_0m_t2	235.87 / 36.56	5.18	10.99	115	0:09:43

Author Manuscript Author Manuscript Author Manuscript Author Manuscript

Test no.	Picture identification parameters	Total dark spot area (cm^2 / $in.^2$)	Percent of dark area	Foam expansion ratio	Drainage accumulation (mL)	Time (hh:mm:ss)
8	B_650fpm_3m_t2	401.53 / 62.24	8.82	11.62	97	0:09:22
	B_650fpm_30m_t2	3,895.95 / 603.87	85.60			
	B_650fpm_0m_t3	108.30 / 16.79	2.38			
	B_650fpm_3m_t3	256.92 / 39.82	5.65			

* Test 13 replaced Test 11 (not shown) due to pictures being obscured by foam.

Author Manuscript Author Manuscript Author Manuscript Author Manuscript

Table 2

ImageJ data for images in Figs. 3, 4, 5 and 6.

Test no.	Image figure no.	Foam agent	Time (min)	Ventilation velocity (m/s)	No-foam area (cm^2 / sq in.)	Area without foam (%)
3	3	A	0	0	4.92 / 0.76	0.11
3	3	A	3	0	36.82 / 5.71	0.81
3	3	A	30	0	267.86 / 41.52	5.88
1	4	B	0	0	37.39 / 5.80	0.82
1	4	B	3	0	164.42 / 25.49	3.61
1	4	B	30	0	3865.22 / 599.11	84.92
13	5	A	0	3.3	73.26 / 11.36	1.61
13	5	A	3	3.3	106.08 / 16.44	2.33
13	5	A	30	3.3	279.06 / 43.26	6.13
6	6	B	0	3.3	31.42 / 4.87	0.69
6	6	B	3	3.3	52.04 / 8.07	1.15
6	6	B	30	3.3	135.41 / 20.99	2.98

Trans Soc Min Metall Explor Inc. Author manuscript; available in PMC 2018 March 19.

Author Manuscript Author Manuscript Author Manuscript Author Manuscript

Trans Soc Min Metall Explor Inc. Author manuscript; available in PMC 2018 March 19.

Table 3

Summary of the image analysis results for blower air foam (PN = printer nozzle; NA = not available).

Test no.	Picture identification parameters	Total dark spot area (cm^2 / sq in.)	Normalized dark spot area (cm^2/ sq in.)	Dark area (%)	Foam expansion ratio	Foam drainage accumulation (mL)	Time (hh:mm:ss)
1b	3D PN 1 _ A_0 fpm_0m	34.75 / 5.39		0.78	16.9	7	00:09:00
	3D PN 1 _ A_0 fpm_3m	81.90 / 12.70		1.83			
	3D PN 1 _ A_0 fpm_30m	238.1 / 36.94		5.33			
8	3D PN1_A_650 fpm_0m_t1	72.60 / 11.22		1.62	13	4	00:08:00
	3D PN1_A_650 fpm_3m_t1	82.20 / 12.74	9.60 / 1.52	1.84			
	3D PN1_A_650 fpm_30m_t1	147.55 / 22.87	74.95 / 11.65	3.30			
1c	3D PN1_A_650 fpm_0m_t2	511.49 / 72.28		11.45	15.7	6	00:08:00
	3D PN1_A_650 fpm_3m_t2	562.41 / 87.17	50.92 / 14.89	12.59			
	3D PN1_A_650 fpm_30m_t2	1,115.32 / 172.88	603.83 / 100.60	24.96			
2a	3D PN1_A_650 fpm_0m_t3	252.94 / 39.21		5.66	12.6	7	00:08:00
	3D PN1_A_650 fpm_3m_t3	338.10 / 52.40	85.16 / 13.19	7.57			
	3D PN1_A_650 fpm_30m_t3	608.33 / 94.29	355.39 / 55.08	13.61			
10	3D PN1_B_0fpm_0m	167.95 / 26.03		3.76	28.2	27	00:08:00
	3D PN1_B_0fpm_3m	300.99 / 46.65		6.74			
	3D PN1_B_0fpm_30m	1617.17 / 250.66		36.19			
4b	3D PN1_B_650 fpm_0m_t1	109.21 / 16.93		2.44	11.6	85	00:08:00
	3D PN1_B_650 fpm_3m_t1	168.55 / 26.13	59.34 / 9.20	3.77			
	3D PN1_B_650 fpm_30m_t1	2,051.09 /317.92	1,941.88 / 300.99	45.90			
4c	3D PN1_B_650 fpm_0m_t2	307.54 / 47.67		6.88	11.9	88	00:08:00
	3D PN1_B_650 fpm_3m_t2	515.04 / 79.83	207.50 / 32.16	11.53			
	3D PN1_B_650 fpm_30m_t2	2,763.05 / 428.27	2,455.51 / 380.60	61.83			
9	3D PN1_B_650 fpm_0m_t3	297.15 / 46.06		6.65	12.1	3	00:08:00
	3D PN1_B_650 fpm_3m_t3	435.83 / 67.55	138.68 / 21.49	9.75			
	3D PN1_B_650 fpm_30m_t3	2,181.56 / 338.14	1,884.41 / 292.08	48.82			
A	3D PN2 _ A_0 fpm_0m	1420.78 / 220.22		31.65	31.3	0	00:10:00
	3D PN2 _ A_0 fpm_3m	1,642.20 / 254.54		36.58			
	3D PN2 _ A_0 fpm_30m	1941.98 / 301.01		43.25			

Author Manuscript Author Manuscript Author Manuscript Author Manuscript

Test no.	Picture identification parameters	Total dark spot area (cm^2 / sq in.)	Normalized dark spot area (cm^2/ sq in.)	Dark area (%)	Foam expansion ratio	Foam drainage accumulation (mL)	Time (hh:mm:ss)
B	3D PN2_A_650 fpm_0m_t1	1,426.71 / 221.14		31.78	35	0	00:10:00
	3D PN2_A_650 fpm_3m_t1	1,684.42 / 261.08	257.71 / 39.94	37.52			
	3D PN2_A_650 fpm_30m_t1	2,366.75 / 366.85	940.04 / 145.71	52.72			
D	3D PN2_A_650 fpm_0m_t2	1,528.00 / 236.84		34.03	26.2	0	00:10:00
	3D PN2_A_650 fpm_3m_t2	1,699.76 / 263.46	171.76 / 26.62	37.86			
	3D PN2_A_650 fpm_30m_t2	2,169.93 / 336.34	641.93 / 99.50	48.33			
C	3D PN2_A_650 fpm_0m_t3	1,690.30 / 262.00		37.65	35.1	0	00:10:00
	3D PN2_A_650 fpm_3m_t3	1,857.50 / 287.91	167.20 / 25.91	41.37			
	3D PN2_A_650 fpm_30m_t3	2,334.38 / 361.83	644.08 / 99.83	51.99			
E	3D PN2_B_0fpm_0m	1,539.91 / 238.69		34.30	50	13	00:10:00
	3D PN2_B_0fpm_3m	1,879.82 / 291.37		41.87			
	3D PN2_B_0fpm_30m	2,029.82 / 314.62		45.21			
F	3D PN2_B_650 fpm_0m_t1	1,775.94 / 275.27		39.56	72.9	7	00:08:00
	3D PN2_B_650 fpm_3m_t1	2,138.07 / 331.40	362.13 / 56.13	47.62			
	3D PN2_B_650 fpm_30m_t1	3,373.77 / 522.94	1,597.83 / 247.67	75.14			
G	3D PN2_B_650 fpm_0m_t2	2,308.20 / 357.77		51.41	51.6	18	00:10:00
	3D PN2_B_650 fpm_3m_t2	2,686.70 / 416.44	378.50 / 58.67	59.84			
	3D PN2_B_650 fpm_30m_t2	4,056.98 / 629.30	1,748.78 / 271.53	90.43			
H	3D PN2_B_650 fpm_0m_t3	2,394.83 / 371.20		53.34	47.3	16	00:08:00
	3D PN2_B_650 fpm_3m_t3	2,820.58 / 437.19	425.75 / 65.99	62.82			
	3D PN2_B_650 fpm_30m_t3	3,661.99 / 567.61	1267.16 / 196.41	81.56			
1a	Brass Nozzle_A_0 fpm_0m	1,454.28 / 225.41		32.54	38.2	1	00:08:00
	Brass Nozzle_A_0 fpm_3m	1,461.16 / 226.48		32.70			
	Brass Nozzle_A_0 fpm_30m	1,650.22 / 255.78		36.93			
1	Brass Nozzle_A_650 fpm_0m_t1	3,166.19 / 490.76		70.85	43.8	0	00:08:00
	Brass Nozzle_A_650 fpm_3m_t1	3,260.68 / 505.41	94.49 / 14.65	72.97			
	Brass Nozzle_A_650 fpm_30m_t1	3,468.55 / 537.63	302.36 / 46.87	77.62			
3	Brass Nozzle_A_650 fpm_0m_t2	1,213.44 / 188.08		27.15	41.7	0	NA
	Brass Nozzle_A_650 fpm_3m_t2	1,275.70 / 197.73	62.26 / 9.65	28.55			
	Brass Nozzle_A_650 fpm_30m_t2	1,726.73 / 267.64	513.29 / 79.56	38.64			

Trans Soc Min Metall Explor Inc. Author manuscript; available in PMC 2018 March 19.

Author Manuscript Author Manuscript Author Manuscript Author Manuscript

Test no.	Picture identification parameters	Total dark spot area (cm^2 / sq in.)	Normalized dark spot area (cm^2/ sq in.)	Dark area (%)	Foam expansion ratio	Foam drainage accumulation (mL)	Time (hh:mm:ss)
3b	Brass Nozzle_A_650 fpm_0m_t3	1,034.28 / 160.31		23.15	36.7	0	NA
	Brass Nozzle_A_650 fpm_3m_t3	1,084.60 / 168.11	50.32 / 7.80	24.27			
	Brass Nozzle_A_650 fpm_30m_t3	1,362.18 / 211.14	327.90 / 50.83	30.48			
4a	Brass Nozzle_B_0 fpm_0m	1,230.94 / 190.80		27.55	51.5	10	00:08:00
	Brass Nozzle_B_0 fpm_3m	1,417.22 / 219.67		31.71			
	Brass Nozzle_B_0 fpm_30m	1,743.37 / 270.22		39.01			
5	Brass Nozzle_B_650 fpm_0m_t1	933.50 / 144.69		20.89	90.5	10	00:15:00
	Brass Nozzle_B_650 fpm_3m_t1	1,127.26 / 174.72	193.76 / 30.03	25.23			
	Brass Nozzle_B_650 fpm_30m_t1	4,468.73 / 692.65	3535.23 / 547.96	100.00			
6	Brass Nozzle_B_650 fpm_0m_t2	1,360.43 / 210.87		30.44	64.8	10	00:10:00
	Brass Nozzle_B_650 fpm_3m_t2	1,538.02 / 238.39	1,77.59 / 27.52	34.42			
	Brass Nozzle_ B_650 fpm_30m_t2	4,454.13 / 690.39	3,093.7 / 479.52	99.67			
7	Brass Nozzle_ B _650 fpm_0m_t3	1,478.02 / 229.09		33.08	48.6	NA	NA
	Brass Nozzle_B_650 fpm_3m_t3	1,565.19 / 242.60	87.17 / 13.51	35.03			
	Brass Nozzle_B_650 fpm_30m_t3	3,944.74 / 611.44	2466.72 / 382.35	88.27			

Trans Soc Min Metall Explor Inc. Author manuscript; available in PMC 2018 March 19.

Author Manuscript Author Manuscript Author Manuscript Author Manuscript

Table 4

Results of *t*-test for roof application face ventilation velocity comparisons (SD = standard deviation).

Time (min)	Foam agent	0 m/s face ventilation airflow average total dark spot area (cm^2 / sq in.)	3.3 m/s (650 fpm) face ventilation airflow average total dark spot area (cm^2 / sq in.)	*t*-test results	Statistically significant?
0	A	39.98 / 6.20	63.89 / 9.90	T(4) = 1.19, p = 0.30	No
		SD = 30.97 / 4.80	SD = 15.42 / 2.39		
3	A	78.92 / 12.14	89.27 / 13.84	T(4) = 0.41, p = 0.70	No
		SD = 41.61 / 6.45	SD = 20.13 / 3.12		
30	A	276.43 / 42.85	239.86 / 37.18	T(2) = 0.91, p = 0.46	No
		SD = 12.13 / 1.88	SD = 55.42 / 8.59		
0	B	162.26 / 25.15	137.35 / 21.29	T(4) = 0.23, p = 0.83	No
		SD = 134.45 / 20.84	SD = 71.61 / 11.10		
3	B	411.87 / 63.84	292.64 / 45.36	T(4) = 0.68, p = 0.53	No
		SD = 235.35 / 36.48	SD = 78.52 / 12.17		
30	B	4,109.15 / 636.92	3,641.48 / 564.43	T(2) = 1.33, p = 0.32	No
		SD = 243.93 / 37.81	SD = 254.52 / 39.45		

Trans Soc Min Metall Explor Inc. Author manuscript; available in PMC 2018 March 19.